Journal of Colloid and Interface Science 442 (2015) 15–21

Contents lists available at ScienceDirect

Journal of Colloid and Interface Science

www.elsevier.com/locate/jcis

Residence time and pH effects on the bonding configuration of orthophosphate surface complexes at the goethite/water interface as examined by Extended X-ray Absorption Fine Structure (EXAFS) spectroscopy

Dalton Belchior Abdala [a,*], Paul Andrew Northrup [b], Flávio César Vicentin [c], Donald Lewis Sparks [d]

[a] Plant & Soil Sciences Department, University of Delaware, Newark, DE 19716, USA
[b] Stony Brook University, National Synchrotron Light Source, Brookhaven National Laboratory, Upton, NY 11973, USA
[c] Brazilian Synchrotron Light Laboratory, Campinas, SP 13083-970, Brazil
[d] Department of Plant & Soil Sciences and Delaware Environmental Institute, University of Delaware, Newark, DE 19716, USA

ARTICLE INFO

Article history:
Received 7 October 2014
Accepted 20 November 2014
Available online 3 December 2014

Keywords:
Phosphorus surface complexation
Adsorption complexes
Phosphorus K-edge EXAFS
P solid-phase speciation

ABSTRACT

Identifying the mechanisms by which P is bound to soils and soil constituents is ultimately important as they provide information on the stability of bound species and their reactivity in the environment. EXAFS studies were carried out to provide information on how the local chemical environment of sorbed P changes as an effect of pH and time. Goethite was reacted with orthophosphate at a P concentration of 0.8 mmol L^{-1} P at pH 3.0, 4.5 and 6.0. The residence time effect on the mechanisms of P sorption on goethite was also evaluated for two different reaction times, 5 and 18 days, on goethite suspensions reacted at pH 4.5. The objective of this study was to understand how P sorption mechanisms change over a wide pH range when subjected to P concentrations above the P saturation ratio of goethite. Phosphorus K-edge EXAFS spectra were collected at 2150 eV in fluorescence mode and the structural parameters were obtained through the fits of sorption data using Artemis. The monodentate surface complex was shown to be the predominant mechanism by which P sorbs at the goethite surface under the experimental conditions. The lack of a discrete Fe–P shell and the presence of highly disordered structures, particularly, at *R*-space $\geqslant$3.5 suggested the formation of P surface precipitates at the goethite/water interface.

1. Introduction

The reactions controlling the fate of oxyanion sorption in soils and soil components are intrinsically dependent upon the interaction between the sorbate species and the sorbent surface, e.g., phosphate (P) and goethite, respectively, and on the pH of the medium and reaction time. This is because pH and contact time between these two entities have a profound effect on the molecular arrangement of the structures formed [1,2], which will, eventually, determine the bioavailability, transport potential and cycling of chemicals in soils [3–5].

Phosphate, an essential plant nutrient and major culprit of eutrophication in fresh waters, is predominantly sorbed in soils by amorphous and crystalline Fe and Al (hydr)oxides through surface complexation or via formation of surface precipitates [6–8]. Goethite (α-FeOOH) is the most common Fe oxide in soils and has the highest P sorption capacity (~2.5 μmol m^{-2}, [7,9]) among the crystalline Fe oxides.

From a macroscopic standpoint, the kinetics of P sorption on goethite is well established, characterized by biphasic kinetics over two time regions [9,10]: an initial rapid reaction followed by slower uptake kinetics which has been attributed, among others, to the formation of surface precipitates of insoluble phosphates at the mineral surface [11] and surface complexation. The latter includes the formation of bidentate binuclear (^{2}C) and monodentate mononuclear (^{1}V) structures [12–17]. Several spectroscopic techniques have been employed to address the sorption mechanisms of P in soils and soil components, primarily, vibrational spectroscopies, particularly IR. This is because the spectral information garnered from this technique represents a fingerprint of the molecular arrangement of a solid with absorption peaks corresponding to the frequencies of vibrations between the bonds of the atoms making up the material being analyzed.

In spite of the versatility of this technique, IR has some limitations in terms of data interpretation caused by the lack of accuracy

* Corresponding author at: Brazilian Synchrotron Light Laboratory, LNLS, Rua Giuseppe Maximo Scolfaro, 10 000 – Campinas, ZIP 13 083-970, SP, Brazil.
E-mail address: dalton.abdala@lnls.br (D.B. Abdala).

http://dx.doi.org/10.1016/j.jcis.2014.11.048
0021-9797/

in determining the exact identity of surface structures that is due to the reliance of molecular assignments on the analytical approach employed [18].

Unlike IR, Extended X-ray Absorption Fine Structure (EXAFS) spectroscopy offers relatively more straightforward information on coordination number, type of nearest neighbors and their distances to the absorbing atom [1,2,4,22]. In addition, it can provide a thorough depiction of interfacial reactions involved in the transition of the surface structures arising at the surface of the solid [19,20].

In light of the great advantages of EXAFS over other spectroscopic techniques, which often require drying and high vacuum, EXAFS spectroscopy has been among the most prominent techniques for studies on the partitioning of heavy metals ions at mineral/water interfaces [21,22]. EXAFS has been widely used in studies on the surface complexation of environmentally relevant elements formed at mineral oxide surfaces and is an effective technique for conducting *in situ* studies addressing, among others, the residence time [1,2,4,23,24] effects on the formation of and differentiation between sorption complexes and surface precipitates.

The environmental conditions at which a certain surface complex is formed have been a matter of debate in spite of the countless number of studies addressing this topic. In order to assist in our discussion throughout this paper, we provide a list of relevant studies on P sorption mechanisms formed at mineral (hydr)oxides surfaces (see Table 1). Based on available literature on this topic, overall, both monodentate and bidentate bonding configurations are formed across a wide pH range (from 3 to approximately 13). With the exception of studies by [14,16,25], one can postulate that a monodentate bonding configuration occurs predominately at higher pHs. On the basis of IR analysis, and as pointed out by Li et al. [26], this could be an artifact due to the protonation state of sorbed P at low pHs, which affects the symmetry of P surface complexes and leads to band splitting. This, consequently, represents a limitation of the IR technique. Persson et al. [14], however, employed *ex situ* FTIR on dried goethite and, as the authors themselves indicate, those two factors may have contributed to significant shifts in band positions, which may have caused inappropriate molecular assignments. Kim & Kirkpatrick [25] also performed their ^{31}P NMR experiments with vacuum-filtered and oven-dried samples. In order to rule out the possible effects that drying could have had on the bonding configuration of P formed on the solid, the authors collected spectra from an undried γ-Al_2O_3 sample reacted with 0.1 M KH_2PO_4 at pH 5. The relatively high P concentration, at which the undried γ-Al_2O_3 reference sample was prepared, could have favored the formation of the monodentate configuration and may have led to the observation of precipitates, even at the lowest P concentrations (10^{-4} mol P). In the work by Rahnemaie et al. [16], MO/DFT calculations were performed to examine the presence of monodentate complexes at low pH without considering the presence of bidentate surface complexes, and that may be the reason why the monodentate complex was predicted under such conditions.

In terms of a bidentate bonding configuration, there seems to exist even more controversy surrounding the conditions at which the formation of such complexes is favored. However, it is believed, based on available literature, that orthophosphate forms only one type of bidentate configuration with (hydr)oxide surfaces, namely corner-sharing or bidentate binuclear (^{2}C) complexation.

The objective of this study was to examine via EXAFS spectroscopy the pH and the residence time effects on P surface complexes formed at the goethite/water interface across a wide pH range and at P concentrations commonly found in soils where P is present in relatively high concentrations, such as in heavily fertilized agricultural soils.

2. Material & methods

2.1. Mineral synthesis

Goethite was synthesized according to Schwertmann & Cornell [39] and is described in detail in [19,20].

Table 1
Relevant studies on the P sorption mechanisms formed at mineral (hydr)oxide surfaces using MO/DFT and ATR-FTIR, CIR-FTIR, NMR and XANES spectroscopies.

Surface complex	Technique	pH	Sorbent	Reference
Monodentate	CIR-FTIR	6–8.4	Goethite	Tejedor-Tejedor & Anderson [13]
	ATR-FTIR	3–13	Goethite	Persson et al. [14]
		>8.5	Hematite	Elzinga & Sparks [32]
		7	Akaganeite	Deliyanni et al., 2007 [46]
	MO/DFT	~12.8	Iron oxides	Kwon & Kubicki, 2004 [35]
		Low pH	Goethite	Rahmenaie et al. [16]
	NMR	3–11	Boehmite, γ-Al_2O_3	Kim & Kirkpatrick [25]
Bidentate	*ex situ* IR	4 and 10	Goethite, hematite, lepidocrocite	Parfitt et al. [29]
	in situ IR	3.6–5.1	Goethite	Parfitt & Atkinson [30]
	CIR-FTIR	<6	Goethite	Tejedor-Tejedor & Anderson [13]
	ART-FTIR	3–8.6	TiO_2	Connor & McQuillan [44]
		4–7.5	Ferrihydrite	Arai & Sparks [42]
		4.5–9	Goethite	Luengo et al. [15]
		<7	Hematite	Elzinga & Sparks [31]
		4.5–9	Nano ferrihydrite	Antelo et al. [41]
	MO/DFT	4–6	Iron oxides	Kwon & Kubicki [35]
		High pH	Goethite	Rahmenaie et al. [16]
	NMR	4–10	Boehmite	Li et al. [26]
		4.5–9	TiO_2	Kang et al. [48]
		3–11	Goethite, akaganeite, lepidocrocite	Kim et al. [17]
		3–11	α-Al_2O_3	Li et al. [50]
	XANES	6	Ferrihydrite	Khare et al. [49]
	XPS	3–13	Goethite	Martin & Smart [52]
Surface precipitates and undetermined inner-sphere bonding configuration	ATR-FTIR	3.3	Corundum	Del Nero et al. [45]
	NMR	4–11	Boehmite	Bleam et al. [43]
		5	Non-xl $Al(OH)_3$	Lookmann et al. [51]
		4–8.5	γ-Al_2O_3	Johnson et al. [47]
		3–11	Boehmite, γ-Al_2O_3	Kim & Kirkpatrick [25]
		3.5–8.5	Kaolinite, gibbsite	Van Emmerick et al. [53]

2.2. Sorption experiments

Goethite was spiked with orthophosphate at a P concentration of 0.8 mM L^{-1}, which is a P concentration equivalent to four times the sorption saturation capacity of goethite (~2.5 μmol m^{-2}, [7,9]) to effect monolayer coverage. Goethite suspensions were reacted with P at the above-mentioned concentration across a wide range of pH, namely 3.0, 4.5 and 6.0. Goethite suspensions at pH 4.5 were also reacted for two different reaction times, 5 and 18 days.

Centrifuge tubes containing stock goethite suspensions of 20 g L^{-1} were placed in a rotating shaker set at 30 rpm at 298 K and equilibrated in 50 mmol L^{-1} KCl with pH adjusted to either 3.0, 4.5 or 6.0 for 36 h prior to phosphate addition. The pH in the suspensions was monitored throughout the shaking period and adjusted to the target pH as needed. Thereafter, an aliquot of the suspension was transferred to a new centrifuge tube to yield a goethite suspension of 2 g L^{-1}, and phosphate solution to yield a P concentration of 0.8 mmol L^{-1} was added. At the end of the agitation period, 5 mL aliquots from each tube were sampled for analysis as described in the following section.

2.3. EXAFS sample preparation and analysis

After sampling, each sample was immediately filtered to pass through a 0.22 μm nitrocellulose membrane filter and washed three times with 3 mL of pH adjusted 50 mmol L^{-1} KCl to remove any entrained phosphate not associated with the surface. The cellulose membrane filter containing the mineral paste was sealed with polypropylene XRF thin film (Ultralene®) and stored moist in a sealed sample box at 6 °C until analysis. Phosphorus K-edge spectra (2150 eV) were collected at beamline SXS at the Brazilian Synchrotron Light Laboratory (LNLS), in Campinas – Brazil, and at Beamline X15B at the National Synchrotron Light Source (NSLS) in Upton, NY – USA. At SXS, EXAFS spectra were collected in fluorescence mode using a silicon drift detector. The beamline was equipped with a monochromator consisting of double crystal Si (1 1 1) and the electron storage ring was operated at 1.37 GeV with a current range of about 110–300 mA [27]. In order to reject higher-order harmonics, one of the monochromator crystals was detuned 45% with respect to the other crystal. At X15B, spectra were collected in fluorescence mode with samples mounted at 45° to the incident beam, using a liquid-nitrogen-cooled Canberra Ultra-Low-Energy Germanium detector positioned at 90°. X15B beamline optics consist of a collimating and harmonic-rejection mirror, a monochromator utilizing Si (1 1 1) crystals to tune energy, and a focusing mirror to gather approximately 5×10^{11} photons s^{-1} into a 1-mm spot at the sample position. The fluorescence signal was normalized to incident beam intensity as measured using a windowless ionization chamber. At either beamlines, EXAFS spectra were collected at photon energies between 2100 and 2800 eV with a minimum step size of 0.1 eV between 2100 and 2155 eV and larger step sizes varying from 0.75 to 6 between 2175 and 2800 eV. Thirteen to eighteen individual spectra were averaged followed by subtraction of the background absorbance through the pre-edge region using the Autobk algorithm [28].

2.3.1. EXAFS data analysis

The averaged spectra were normalized to an atomic absorption of one, and the EXAFS signal was extracted from the raw data using linear pre-edge and a quadratic spline post-edge. The data were converted from energy to photoelectron momentum (k-space) and k-weighted by k^2. EXAFS spectra were calculated over a typical k-space range with a Hanning window and 0.5 width Gaussian wings. Fourier transforms (FT) of the k^2-weighted EXAFS were calculated over a k-range between 10.3 and 10.6 and performed to obtain the R-space. Structural information was obtained by fitting Fourier transformed EXAFS data with ARTEMIS [40]. The FT of the EXAFS was fit with the predicted function by varying the number of coordinating atoms (CN), their distance (ΔR), mean square displacement (δ^2) and passive electron reduction factor (S_0^2) in order to obtain the best fit between the experimental and predicted spectra.

A more detailed description of the fitting and data analysis can be found in Abdala et al. [20].

3. Results & discussion

Studies addressing P sorption mechanisms on Fe and Al (hydr)oxides, particularly on goethite, have resulted in countless conflicting interpretations of binding mechanisms. It is not unusual to find studies indicating that bidentate and monodentate configurations have been assigned to the formation of a phosphate surface complex under similar experimental conditions (Table 1).

Previous studies employing spectroscopic techniques to characterize phosphate surface complexes forming on (hydr)oxide mineral surfaces include MO/DFT, ATR-FTIR, CIR-FTIR, NMR and XANES spectroscopies. Unlike the above-mentioned spectroscopic techniques, EXAFS analysis is able to provide detailed information on the local coordination environment of an atom, such as interatomic distances, identity of nearest neighbors and coordination numbers. The discussion that follows will be focused on the orthophosphate bonding configurations on the basis of interatomic distances and coordination numbers found within our orthophosphate/goethite systems.

3.1. P-EXAFS spectra

Fig. 1 shows the Fourier Transform of experimental $\chi(k)$ spectra of goethite spiked with P at a P concentration of 0.8 mmol L^{-1} at pH 3.0, 4.5 and 6.0. Fig. 2 shows the Fourier Transform of experimental $\chi(k)$ spectra of goethite spiked with P at pH 4.5 at 5 and 18 days reaction time. Figs. 3 and 4 show the experimental $\chi(k)$ spectra and corresponding best fit of goethite spiked with P at a P concentration of 0.8 mmol L^{-1} at pH 3.0, 4.5 and 6.0 and of goethite spiked with P at pH 4.5 at 5 and 18 days reaction time, respectively. The peaks shown in the experimental $\chi(k)$ spectra correspond to the coordination shells formed between P–O and P–Fe and reflect the interatomic distances within the material. For all samples, the E_0 ranged from 0.79 to 3.6 eV. The contributions of O were localized at P–O distances ranging from 1.51 to 1.54, being longer at the lowest pH, 1.54 Å, intermediate at pH 4.5, 1.53 Å, and shorter at pH 6.0, 1.51 Å, and MS dominated at ~2.75–2.79 Å. The P–Fe shells indicated the existence of two predominant bonding configurations between P and the goethite surface, bidentate binuclear and monodentate mononuclear (see Figs. 2–4).

3.2. Overall formation of P surface complexes at the goethite/water interface

Two different phosphate surface complexes were identified at the goethite/water interface at the experimental conditions investigated, namely bidentate binuclear (^{2}C) and monodentate mononuclear (^{1}V) surface complexes. Additionally, analyses of the Fourier transforms of sorption data suggests that surface precipitates were also present across all samples analyzed in our study.

The shortest P–Fe distances of 3.23, 3.27 and 3.26 Å were characteristic of a bidentate binuclear configuration between P and Fe across the pH range in our study, 3.0, 4.5 and 6.0, respectively. The most distant shells, occurring at ~3.59, 3.53 and 3.58 Å were indicative of a monodentate configuration between P and Fe. Table 2

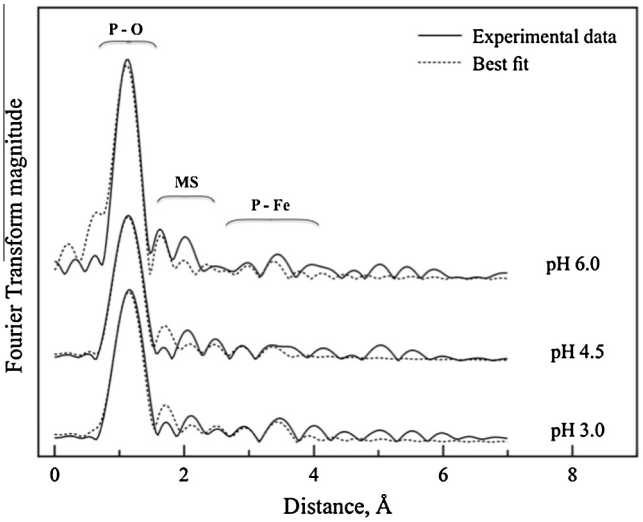

Fig. 1. Fourier transformed spectra of experimental (solid line) and best fit (dashed line) of the phosphate surface complexes formed at the goethite/water interface at pH 3.0, 4.5 and 6.0. A change in spectrum shape (*R*-space) as a result of increasing pH from pH 3.0 to 6.0 indicates that the phosphate surface speciation is sensitive to pH. Braces are intended to show the approximate region where the P–O, MS and P–Fe shells most significantly contribute in radial distance in the Fourier transformed spectra.

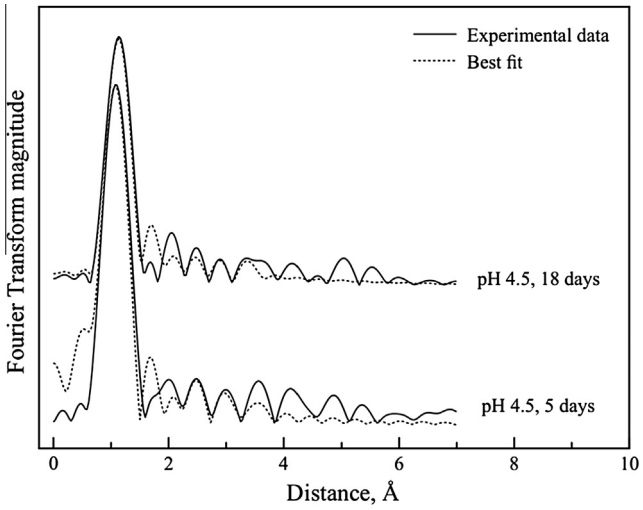

Fig. 2. Fourier transformed spectra of experimental (solid line) and best fit (dashed line) of the phosphate surface complexes formed at the goethite/water interface at pH 4.5 at 5 and 18 days reaction time. Braces are intended to show the approximate region where the P–O, MS and P–Fe shells most significantly contribute in radial distance in the Fourier transformed spectra.

shows the, P–O and P–Fe bonding distances and corresponding P sorption mechanisms across the pH range in our study. In terms of reaction time effects on P bonding configurations, no changes in the predominance of a surface complex over another were observed. However, our results showed that aging had a rather pronounced effect on bond lengths, suggesting that longer contact times favor shorter bond lengths, as evidenced by a shorter P–O bond at goethite reacted for 18 days, 1.51 Å, in comparison with a longer P–O bond of 1.53 Å for goethite reacted with orthophosphate for 5 days. On the basis of P–Fe bond lengths, residence time showed an even more significant effect on bond lengths, shortening P–Fe distances by as much as 0.7 Å on both surface complexes (Table 3).

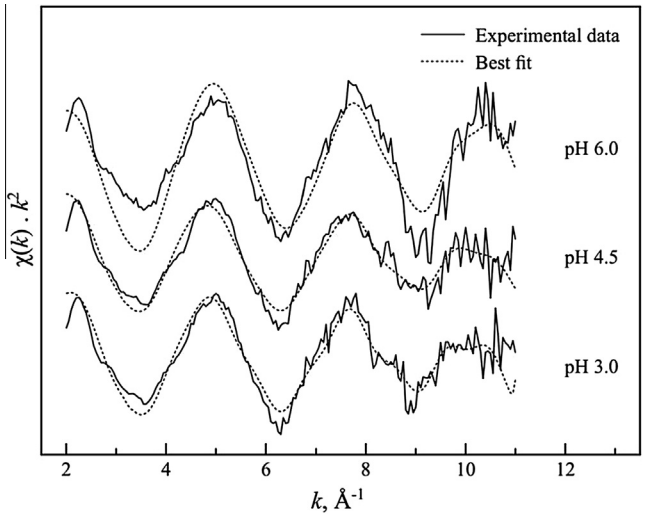

Fig. 3. Experimental (solid line) and best-fit (dashed line) k^2-weighted back transformed spectra of phosphate sorbed on goethite at pH 3.0, 4.5 and 6.0.

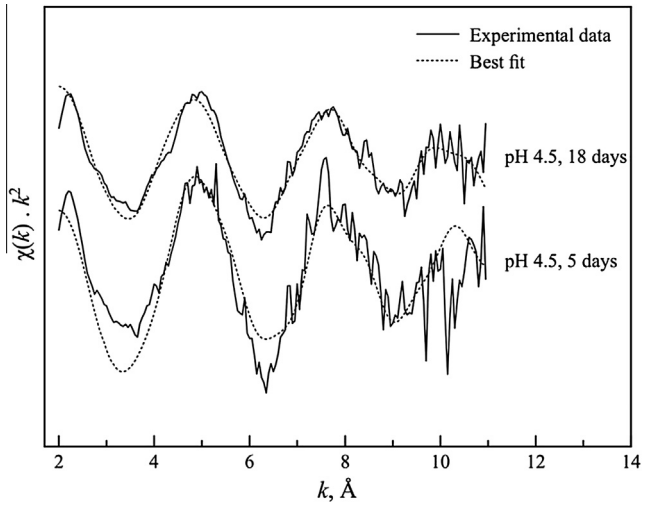

Fig. 4. Experimental (solid line) and best-fit (dashed line) k^2-weighted back transformed spectra of phosphate sorbed on goethite at pH 4.5 at 5 and 18 days reaction time.

3.3. Adsorption complexes

As indicated in Table 2, our results show that bidentate and monodentate surface complexes were present in all samples regardless of pH and reaction times. However, as indicated by the amp (S_0^2) values, a higher contribution of monodentate configuration was experienced at lower pHs that progressively decreased as pH increased from 3.0 to 6.0. The bidentate configuration was a minor contribution in the *R*-space, however, a bidentate path improved the fits significantly. This seems consistent with the literature that indicated that low surface coverages favor the formation of bidentate surface complexes [13,16,25,29,30,12,31] and that the relative importance of bidentate binuclear species decreases as surface loading increases such that a monodentate configuration would predominate at higher surface loadings [13,16]. Antelo et al. [32,33], on the basis of ATR-FTIR, have observed that P adsorbs mainly as bidentate complexes at high phosphate loadings and that monodentate surface complexes begin to be important at low phosphate loadings and at high pHs. This was ascribed to bidentate species locating more charge

Table 2
P–O and P–Fe bonding distances, surface complex distribution and corresponding bonding configurations of P on goethite at three different pHs.

pH	P–O			P–Fe					
				Bidentate			Monodentate		
	R Å	σ^2	S_0^2	R Å	σ^2	S_0^2	R Å	σ^2	S_0^2
3.0	1.54 (±0.004)	0.0014 (±0.0007)	0.79 (±0.045)	3.23 (±0.07)	0.01 (±0.006)	0.38 (±0.04)	3.59 (±0.03)	0.0014 (±0.004)	1.04 (±0.25)
4.5	1.53 (±0.005)	0.0018 (±0.0007)	0.75 (±0.045)	3.27 (±0.06)	0.0012 (±0.008)	0.16 (±0.015)	3.53 (±0.04)	0.0053 (±0.007)	0.76 (±0.33)
6.0	1.51 (±0.007)	0.0001 (±0.0001)	0.85 (±0.07)	3.26 (±0.06)	0.008 (±0.03)	0.26 (±0.03)	3.58 (±0.09)	0.004 (±0.01)	0.72 (±0.21)

R: radial structure function (RSF); σ^2: mean square displacement, S_0^2: passive electron reduction factor, (): uncertainties associated with parameter estimates.

Table 3
P–O and P–Fe bonding distances, surface complex distribution and corresponding bonding configurations of P on goethite at two different reaction times.

Reaction time	P–O			P–Fe					
				Bidentate			Monodentate		
	R	σ^2	S_0^2	R	σ^2	S_0^2	R	σ^2	S_0^2
Days	Å			Å			Å		
5	1.51 (±0.004)	0.0004 (±0.0009)	0.92 (±0.054)	3.30 (±0.05)	0.0002 (±0.005)	0.30 (±0.12)	3.6 (±0.04)	0.003 (±0.002)	1.04 (±0.31)
18	1.53 (±0.005)	0.0018 (±0.0007)	0.75 (±0.045)	3.27 (±0.06)	0.0012 (±0.008)	0.16 (±0.015)	3.53 (±0.04)	0.0053 (±0.007)	0.76 (±0.33)

R: radial structure function (RSF); σ^2: mean square displacement, S_0^2: passive electron reduction factor, (): uncertainties associated with parameter estimates.

at the surface than monodentate species, producing a lower electrostatic repulsion between the adsorbed species in the 1-plane. Interestingly, the observation of [32,33] is consistent with the behavior of arsenic in its pentavalent form (As(V)), an analog of phosphate, having similar chemical and geometric properties, and present as the ionic species, $H_2AsO_4^-$ and $H_2PO_4^-$, respectively, at the typical pH range in the environment.

3.3.1. Bidentate binuclear configuration

A bidentate binuclear configuration (^{2}C) of phosphate on (hydr)oxides has been shown in the literature to exist over a wide range of pH (Table 1 in Abdala et al. [20]). In this study, the ^{2}C surface complex was present, although at different proportions, across the entire pH range in the study. As discussed in Abdala et al. [20], a bidentate configuration should be expected to predominate at lower surface coverages as that configuration should be favored when the Fe/P ratio is smaller than unity. It follows that at low P concentration, the sorption sites compete with the PO_4 molecules at the same strength such that one PO_4 molecule must equally satisfy as many sorption sites as possible. Therefore, ^{2}C forms first and because it is strongly bound to high affinity sorption sites, it has a large thermodynamic stability, thus remaining associated with the surface even as solution P concentration increases. The higher proportion of a ^{2}C configuration was found to be in good agreement with the proposal by [34] that at low pHs, a higher positive surface charge induces a higher adsorption capacity for anions like phosphate, because more negative charge can be brought to the surface for a given change in electrostatic potential.

Table 3 shows the surface complex distribution as a function of pH.

3.3.2. Monodentate configuration

Overall, our results showed that a monodentate species is dominant over a broad pH range and high surface loadings whereas a bidentate species is particularly important at low pHs.

Our results were in good agreement with the relatively few spectroscopic studies that have reported P being attached to (hydr)oxide surfaces in a monodentate (^{1}V) configuration (Table 1). The studies in which a ^{1}V configuration has been observed were, in general, carried out employing P concentrations at relatively high surface coverages [13,31]. Residence time had a marked effect on bond lengths, with a P–Fe distance of 3.59 Å for goethite reacted for 5 days and 3.53 Å when reaction time was extended to 18 days.

Whereas the P–Fe distances for bidentate binuclear configuration are in good agreement with the work by Rahnemaie et al. [16], who found P–Fe distances varying between 3.22 and 3.26 Å, the P–Fe distance for a monodentate configuration observed in our study was much larger, varying from 3.53 to 3.59 Å. However, they are in agreement with the calculations performed by Kwon & Kubicki [35], who found P–Fe bond distances generally longer for either configuration, if a $\geqslant$170° angle is formed by P–O–Fe, suggesting a P–Fe bond distance of around 3.6 Å. EXAFS studies indicate that for As(V) these distances are generally in the order of 3.57–3.63 Å [36,22]. Since P is a much lighter element than As, it is possible that the repulsion of P by the Fe atoms tend to maintain P as farther apart from Fe as possible, thus P–O–Fe forms preferentially a linear structure when a monodentate configuration is formed. Alternatively, the Fe–O bond distance may also be influenced by repulsion and, accordingly, resulting in a longer total Fe–P distance.

3.4. Surface precipitate formation

The transition point from adsorption (or monolayer surface coverage) to precipitation (multilayer coverage or the formation of a separate phase) is not clearly defined [37]. Torrent et al. [9] estimated that, for monolayer coverage, the maximum P adsorption at the goethite surface should be 5 μmol m^{-2} for mononuclear bonding or 2.5 μmol m^{-2} for binuclear bonding. On the basis of their calculation, surface precipitates should have been observed at the two highest P loadings in our study. According to Dzombak

& Morel [38], the dissolution of iron from the mineral (hydr)oxide is a limiting factor for surface precipitation to occur, since surface precipitates are formed at the expense of dissolved material from the adsorbent surface. This might be the reason for the small degree of surface precipitation observed, given the relatively high phosphate loading employed in this study.

We observed surface precipitates in our study based on calculations performed to the overall amplitude and the individual fractions of P in each bonding configuration, in which we considered the relative distribution of monodentate and bidentate binuclear surface complexes. Additionally, the presence of some modulation of short-range ordered structure, appearing at high R-space values ($\geqslant$3.5 Å), associated with the lack of a discrete Fe shell, was interpreted as an indication of the formation of highly disordered surface precipitate structures.

3.5. Environmental implications of our findings

The establishment of environmentally sound P management practices relies on the identification of soil P retention and release mechanisms. Molecular descriptions of phosphate retained on mineral surfaces is important because they allow one to precisely model the P sorption process, to determine the stability of the surface complex being formed and, ultimately, to predict the fate of P in the environment. Observations in this study show that the local coordination environment of P is sensitive to changes in soil pH and reaction time, lending further evidence that at lower pHs, P is more tightly retained by goethite via a bidentate bridging surface complex, exhibiting the shortest bond lengths at the lowest pH studied and that bond lengths progressively increase as an increase in pH occurs. These findings corroborate macroscopic observations that in more acidic soils P availability is limited, presumably due to energetic constraints imparted by the formation of a more thermodynamically stable surface complex even at high P surface loadings, exceeding monolayer formation (0.8 μmol m^{-2}). On the other hand, a monodentate configuration would be the predominant surface complex at higher pHs, particularly at higher P loadings [20]. Therefore, in a typical agricultural scenario, where soils are consecutively fertilized with P, whether in organic forms, e.g., manures, or in inorganic forms, e.g., mineral fertilizers, soil pH is generally raised due to liming for crop cultivation and, under such circumstances, the higher pHs may favor the release of P [54]. In addition, our observations suggest that P loss potential should be greater following fertilization and, as time proceeds, attenuation in P loss should be expected as a result of longer contact between P and the soil mineral surfaces.

3.6. Final remarks and scientific achievements obtained in this study

We have successfully showed the applicability of EXAFS spectroscopy to shed light on the mechanisms by which P sorbs onto goethite across a wide pH range, relatively high surface loadings and reaction times.

Accordingly, the monodentate complex was observed across the entire pH range in the study, indicating that pH does not seem to play a major role in surface complexation under the experimental conditions in which this study was carried out. The bidentate binuclear surface complex was also observed, particularly at lower pHs. It is important to mention that while the EXAFS spectra are dominated by monodentate bonding configuration, the presence of the bidentate complex shows that, regardless of environmental conditions, e.g., pH, surface loading and residence time, its formation is thermodynamically favorable [20]. It is also important to note that, even though the bidentate complex contribution is small, the dominance of the monodentate complex signal in the EXAFS spectra represents the 'average' local environment of P.

In general agreement with the literature on residence time effects on P surface complexation, the P adsorption process took place as part of two interconnected processes, a very fast initial process, which seemed to take place in time-scales of minutes resolution or less, followed by a slower process that took place over hours or even days [10,11,15]. Therefore, at the time-scale at which our experiments were performed, one should not expect to observe major changes in the surface complexes being formed other than effects on bonding distances. However, residence time had an effect on P–Fe distances, with longer exposure times resulting in shorter P–Fe distances for both monodentate and bidentate surface complexes. The shortening of P–Fe distances as reaction time increases seems to reflect some sort of instability of both surface complexes at short reaction times. The formation of shorter P–Fe bond distances at extended reaction times suggest that both surface complexes become more stable as they are located closer to the surface. This suggests, therefore, that shorter exposure times may favor a greater reversibility of phosphate.

The ubiquitous presence of some modulation of short-range ordered structure, appearing at high R-space values ($\geqslant$3.5 Å) associated with the lack of a discrete Fe shell could be an indication of formation of highly disordered structures, such as surface precipitates.

3.7. A synopsis on new concepts and a vision for future studies employing EXAFS spectroscopy to study phosphorus reactions in natural systems

Although very useful information can be obtained from P K-edge XANES spectroscopy [49,55–58], analysis of P K-edge XANES data provides limited information on the local atomic environment of P [56]. Thus, P K-edge XANES is primarily used as a "fingerprint" technique [56–59]. Unlike P K-edge XANES, EXAFS analysis of P can provide additional structural information on the local environment of such an important element not only with respect to (i) its interaction with soil components, but also (ii) on the molecular assignments of P in biological tissues and (iii) in the development of P fertilizers, as it can allow one to observe the structural changes in the P containing fertilizer products upon fertilizer dissolution.

Since EXAFS spectroscopy can provide direct observations on the local environment of an element, many questions relative to the bonding mechanisms of P in soils can now be gleaned via P-EXAFS analysis. Below, we provide a group of studies on the chemistry of P in soils in which the use of P-EXAFS spectroscopy could be advantageous.

Addressing P surface complexation in soils is undoubtedly the greatest analytical barrier to overcome in using this technique to study the chemistry of P in soils. This is because of the presence of sulfur (S) in environmental samples, which makes it a drawback to use P-EXAFS in natural soils. Small though it might be, the appearance of a S K-edge at around 2470–2482 eV (depending on the oxidation state of S present in the sample) impacts the collection of a useful P-EXAFS spectrum. However, as the present study shows, P-EXAFS spectroscopy can effectively be employed in studies where model analogues of soil minerals are used to address mechanistic aspects of the chemistry of soil P. Future microbeam EXAFS facilities such as under development at NSLS-II 8-BM will further enable isolation of more pure domains within heterogeneous soils.

Likewise, P-EXAFS studies can provide a more detailed and straightforward understanding about the competitive sorption aspects of widely known and environmentally relevant elements that strongly competes with P in soils, such as Arsenic [60–62]. Similarly, P-EXAFS analysis will enable one to make direct observations on the effects of low-molecular-weight organic acids on P sorption (and vice versa) in soils [63,64].

Another application is the capability to examine the effects of plant available extractant solutions on P surface complexes, with particular emphasis on the desorption order of P upon interaction with the extractant solution as well as on how the conformational structure of P surface complexes changes following interaction with extractants.

Improvements on our understanding on the partitioning of P in artificial soils, obtained from mineral mixtures, might also be achieved and will help us to determine the effect of a given extractant solution on the desorption of a particular P species in sequential P chemical fractionation procedures.

The chemistry of organic phosphorus in soils, particularly with respect to organic P reactions with organic and inorganic constituents present in the rhizosphere, may be better understood using P EXAFS analysis.

Acknowledgments

The senior author gratefully acknowledges the receipt of a Delaware Environmental Institute (DENIN) graduate fellowship. The authors appreciate financial support from the U.S. National Science Foundation via Delaware EPSCoR. Support for this project was made possible by the Unidel Foundation and by Delaware EPSCoR with funds from the National Science Foundation Grant EPS-0814251. We also extend our thanks to the National Synchrotron Light Source and to the Brazilian Synchrotron Light Laboratory for providing the technical support and the conditions for carrying out our research.

References

[1] S.E. O'Reilly, D.G. Strawn, D.L. Sparks, Soil Sci. Soc. Am. J. 65 (2001) 67–77.
[2] Y. Arai, D.L. Sparks, Soil Sci. 167 (2002) 303–314.
[3] J.J. Pignatello, B. Xing, Environ. Sci. Technol. 30 (1996) 1–11.
[4] A.M. Scheidegger, D.G. Strawn, G.M. Lamble, D.L. Sparks, Geochim. Cosmochim. Acta 62 (1998) 2233–2245.
[5] D.G. Strawn, A.M. Scheidegger, D.L. Sparks, Environ. Sci. Technol. 32 (1998) 2596–2601.
[6] J.R. McLaughlin, J.C. Ryden, J.K. Sayers, J Soil Sci. 32 (1981) 365–377.
[7] O.K. Borggaard, J. Soil Sci. 34 (1983) 333–341.
[8] R.L. Parfitt, J. Soil Sci. 40 (1989) 359–369.
[9] J. Torrent, Aust. J. Soil Res. 29 (1991) 69–74.
[10] N.J. Barrow, Adv. Agron. 38 (1985) 183–230.
[11] J. Torrent, U. Schwertmann, V. Barrón, Clays Clay Miner. 40 (1992) 14–21.
[12] R.L. Parfitt, J.D. Russell, J. Soil Sci. 28 (1977) 297–305.
[13] M.I. Tejedor-Tejedor, M.A. Anderson, Langmuir 6 (1990) 602–611.
[14] P. Persson, N. Nilsson, S. Sjoberg, J. Colloid Interface Sci. 177 (1996) 263–275.
[15] C. Luengo, M. Brigante, J. Antelo, M. Avena, J. Colloid Interface Sci. 300 (2006) 511–518.
[16] R. Rahnemaie, T. Hiemstra, W.H. van Riemsdijk, Langmuir 23 (2007) 3680–3689.
[17] J. Kim, W. Li, B.L. Philips, C.P. Grey, Energy Environ. Sci. 4 (2011) 4298–4305.
[18] Y. Arai, D.L. Sparks, Adv. Agron. 94 (2007) 135–179.
[19] D.B. Abdala, On the Use of Extended X-Ray Absorption Fine Structure (EXAFS) Spectroscopy to Determine the Bonding Configuration of Orthophosphate Surface Complexes at the Goethite/Water Interface. University of Delaware, Newark, 2013 (PhD. Thesis).
[20] D.B. Abdala, P.A. Northrup, D.L. Sparks, J. Colloid Interface Sci. 437 (2015) 297–303.
[21] A.M. Scheidegger, G.M. Lamble, D.L. Sparks, J. Colloid Interface Sci. 186 (1997) 118–128.
[22] S.E. Fendorf, M.J. Eick, P.R. Grossl, D.L. Sparks, Environ. Sci. Technol. 31 (1997) 315–320.
[23] L. Charlet, A. Manceau, J. Colloid Interface Sci. 148 (1992) 443–458.
[24] B.A. Manning, S.E. Fendorf, S. Goldberg, Environ. Sci. Technol. 32 (1998) 2383–2388.
[25] Y. Kim, R.J. Kirkpatrick, Eur. J. Soil Sci. 55 (2004) 243–251.
[26] W. Li, J. Feng, K.D. Kwon, J.D. Kubicki, B.L. Phillips, Langmuir 26 (2010) 4753–4761.
[27] M. Abbate, F.C. Vicentin, V. Compagnon-Cailhol, M.C. Rocha, H.J. Tolentino, Synchr. Rad. 6 (1999) 964–972.
[28] M. Newville, P. Livins, Y. Yacoby, J.J. Rehr, E.A. Stern, Phys. Rev. B Condens. Matter 47 (1993) 14126–14131.
[29] R.L. Parfitt, Atkinson, R.St.C. Smart, Soil Sci. Soc. Am. J. 39 (1975) 837–841.
[30] R.L. Parfitt, R.J. Atkinson, Nature 264 (1976) 740–742.
[31] E.J. Elzinga, D.L. Sparks, J. Colloid Interface Sci. 308 (2007) 53–70.
[32] J. Antelo, M. Avena, S. Fiol, R. Lopez, F. Arce, J. Colloid Interface Sci. 285 (2005) 476–486.
[33] J. Antelo, S. Fiol, C. Pérez, S. Mariño, F. Arce, D. Gondar, R. López, J Colloid Interface Sci. 347 (2010) 112–119.
[34] T. Hiemstra, Surface complexation at mineral interfaces: Multisite and Charge Distribution approach. (Ph.D. thesis), Wageningen University, 2010.
[35] K.D. Kwon, J.D. Kubicki, Langmuir 20 (2004) 9249–9254.
[36] G.A. Waychunas, B.A. Rea, C.C. Fuller, J.A. Davis, Geochim. Cosmochim. Acta 57 (1993) 2251–2269.
[37] R.B. Corey, Adsorption vs. coprecipitation, in: M.A. Anderson, A.J. Rubin (Eds.), Adsorption of Inorganics at Solid–Liquid Interfaces, Ann Arbor Science, Ann Arbor Mich, 1981, pp. 161–182.
[38] D.A. Dzombak, F.M.M. Morel, Surface Complexation Modeling: Hydrous Ferric Oxide, Wiley-Interscience, New York, 1990, p. 393.
[39] U. Schwertmann, R.M. Cornell, Iron Oxides in the Laboratory: Preparation and Characterization, Wiley-VCH, Weinheim, Germany, 2000.
[40] B. Ravel, M. Newville, J. Synchrotron Rad. 12 (2005) 537–541.
[41] J. Antelo, F. Arce, M. Avena, S. Fiol, R. Lopez, F. Macias, Geoderma 138 (2007) 12–19.
[42] Y. Arai, D.L. Sparks, J. Colloid Interface Sci. 241 (2001) 317–326.
[43] W.F. Bleam, P.E. Pfeffer, S. Goldberg, R.W. Taylor, R. Dudley, Langmuir 7 (1991) 1702–1712.
[44] P.A. Connor, A.J. McQuillan, Langmuir 8 (1999) 2916–2921.
[45] M. Del Nero, C. Galindo, R. Barillon, E. Halter, B. Madé, J. Colloid Interface Sci. 342 (2010) 437–444.
[46] E.A. Delyianni, E.N. Peleka, N.K. Lazaridis, Sep. Purif. Technol. 58 (2007) 478–486.
[47] B.B. Johnson, A.V. Ivanov, O.N. Antzutkin, W. Forsling, Langmuir 18 (2002) 1104–1111.
[48] S.A. Kang, W. Li, H.E. Lee, B.L. Phillips, Y.J. Lee, J. Colloid Interface Sci. 364 (2011) 461–465.
[49] N. Khare, J.D. Martin, D. Hesterberg, Geochim. Cosmochim. Acta 71 (2007) 4405–4415.
[50] W. Li, X. Wenqian, J.B. Parise, B.L. Phillips, Geochim. Cosmochim. Acta 85 (2012) 289–301.
[51] R. Lookmann, P. Grobet, R. Merckx, K. Vlassak, Eur. J. Soil Sci. 45 (1994) 37–44.
[52] R.R. Martin, R.St.C. Smart, Soil Sci. Soc. Am. J. 51 (1987) 54–56.
[53] T.J. Van Emmerick, D.E. Sandstrom, O.N. Antzutkin, M.J. Angove, B.B. Johnson, Langmuir 23 (2007) 3205–3213.
[54] D.B. Abdala, A.K. Ghosh, I.R. Silva, R.F. Novais, V.V.H. Alvarez, Agric. Ecosys. Environ. 162 (2012) 15–23.
[55] W. Negassa, J. Kruse, D. Michalik, N. Appathurai, L. Zuin, P. Leinweber, Environ. Sci. Technol. 44 (2010) 2092–2097.
[56] D. Hesterberg, Macro-scale chemical properties and X-ray absorption spectroscopy of soil phosphorus, in: B. Singh, M. Gräfe (Eds.), Synchrotron-based techniques in soils and sediments. Developments in Soil Science, 2010, pp. 313–356.
[57] J. Brandes, E. Ingall, D. Paterson, Mar. Chem. 103 (2007) 250–265.
[58] E.D. Ingall, J.A. Brandes, J.M. Diaz, M.D. de Jonge, D. Paterson, I. McNulty, W.C. Elliot, P. Northrup, J. Synchrotron. Radiat. 18 (2011) 189–197.
[59] J. Liu, J. Yang, X. Liang, Y. Zhao, B. Cade-Menun, Y. Hu, Soil Sci. Soc. Am. J. 78 (2014) 47–53.
[60] B. Manning, S. Goldberg, Soil Sci. Soc. Am. J. 60 (1996) 121–131.
[61] A. Violante, M. Pigna, Soil Sci. Soc. Am. J. 66 (2002) 1788–1796.
[62] H.M. Selim, Competitive sorption of heavy metals in soils: experimental evidence, in: H. Magid Selim (Ed.), Competitive Sorption and Transport in of Heavy Metals in Soils and Geological Media, CRC Press, 2013, pp. 1–48.
[63] N.S. Bolan, R. Naidu, S. Mahimairaja, S. Baskaran, Biol. Fertil. Soils 18 (1994) 311–319.
[64] M. Lindegren, P. Persson, Eur. J. Soil Sci. 60 (2009) 982–993.